

## REDOX TREATMENT OF AN Fe/Al PILLARED MONTMORILLONITE. A MÖSSBAUER STUDY

T. BAKAS,<sup>1,\*</sup> A. MOUKARIKA,<sup>1</sup> V. PAPAETHYMIU,<sup>1</sup> AND A. LADAVOS<sup>2</sup>

<sup>1</sup> Physics Department, The University of Ioannina, GR 451 10 Ioannina, Greece

<sup>2</sup> Chemistry Department, The University of Ioannina, GR 451 10 Ioannina, Greece

**Abstract**—Pillared structures with an interlayer opening of ~0.3 nm were obtained after successive heat treatments of the PILC precursor in reducing and oxidizing conditions. This precursor was prepared by reacting a Na<sup>+</sup>-montmorillonite with an intercalant containing Al and Fe oxo-hydroxides (Al/Fe = 1). Powder X-ray diffraction, elemental analysis, <sup>57</sup>Fe Mössbauer spectroscopy, catalytic activity measurements and surface area data were used to characterize the samples. On the basis of Mössbauer spectra taken at temperatures between 4.2 and 300 K, it is deduced that oxidizing steps produce Al substituted maghemite which converts into Al substituted magnetite upon reducing heat treatment. Firing the precursor in oxidizing atmosphere forms pillars of few nm in diameter. However, heating under reducing conditions yields pillars of smaller diameter. This later behaviour is maintained even after reheating the material in oxidizing atmosphere. From the temperature dependence of Mössbauer spectra it is deduced that the diameter of the Fe oxide particles in the pillars is smaller than 10 nm.

**Key Words**—Lepidocrocite, Maghemite, Magnetite, Modified montmorillonite, Mössbauer, PILC, Superparamagnetism.

### INTRODUCTION

Pillared layered clays (PILCs) constitute a novel class of microporous materials with a thermal stability up to about 700°C, a surface area in the range of 200 to 500 m<sup>2</sup>/g and a pronounced Bronsted and Lewis acidity (Brindley and Sempels, 1977; Pinnavaia, 1983; Fripiat, 1986; Bergaya and Barrault, 1990). These materials result from a two-step modification of naturally occurring or synthetic swelling clay minerals, i.e., smectites. The first step comprises the propping apart of the clay layers by intercalating with oligo- or polymeric cationic complexes of metals, as e.g., (Al<sub>13</sub>O<sub>4</sub>(OH)<sub>24</sub>-(H<sub>2</sub>O)<sub>12</sub>)<sup>7+</sup> in the clay interlayer space. At the second step, upon calcining this precursor material at 500°C, the inserted complexes transform into nano-sized pillars of metal oxides cross-linked to the silicate layers. Thus, the structure of PILCs can be envisaged as a stacking of two dimensional networks of pores with sizes in the nanometer range. Clearly, PILCs present a class of novel host materials for molecular sorption, chemical synthesis and catalysis. The steric and electronic constraints prevailing in this super-zeolitic structure (Vaughan, 1988) render to these novel materials a high selectivity. The list of metal oxides used in pillaring various smectites has rapidly expanded and already comprises quite a few metals, e.g., Al (Lahav *et al.*, 1978), Zr (Bartley, 1988), Si (Endo *et al.*, 1980),

Cr (Tzou and Pinnavaia, 1988), Fe (Yamanaka *et al.*, 1984), Ti (Sterte, 1986), Nb and Ta (Christiano *et al.*, 1985), Mo (Christiano and Pinnavaia, 1986), Sn (Petridis *et al.*, 1989). Furthermore, the synthetic route to PILCs shows a new way to engineer out of swelling clays a multitude of nanophases. This presents a new challenge from a materials' science point of view (Mitchell, 1990).

The early recognition that PILCs have important potential applications as catalysts, sorbents, sensors, etc. (Vaughan and Lussier, 1980; Ocelli, 1983; Bergaya *et al.*, 1991) has stimulated research not only for the synthesis of new PILCs, but also for their extensive microscopic characterization. A wide spectrum of analytical techniques, e.g., magic-angle spinning NMR (Plee *et al.*, 1985; Tillak *et al.*, 1986), EPR (Harsh and Doner, 1984; Braddell *et al.*, 1987), neutron scattering (Pinnavaia *et al.*, 1984), NMR and H<sub>2</sub>TPR (Bergaya *et al.*, 1993) and Mössbauer spectroscopy (Gangas *et al.*, 1985; Lee Woo *et al.*, 1989; Petridis *et al.*, 1989), has been used for unravelling the structure and the properties of these novel materials. However, in spite of the substantial advance made up to now in the synthesis and characterization of PILCs, the elucidation of additional aspects of the pillared structure (e.g., the diameter of the pillars) is of cardinal importance for understanding the role of their morphology in physicochemical processes occurring in the interlayer space, as well as developing applications.

In this paper we present the findings of a study that aimed at the elucidation of the composition and mor-

\* Address correspondence to T. Bakas.

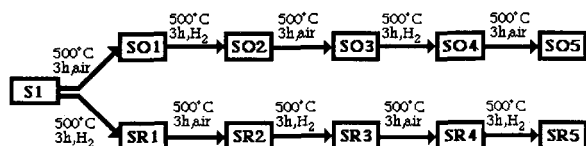


Figure 1. Diagram depicting the redox cycles imposed on the PILC precursor sample (S1) and the samples obtained after each cycle.

phology of the iron phases in: 1) two pillared clay structures gained from the same PILC-precursor after heating either under oxidizing or reducing conditions; and 2) these two PILCs after cyclic oxidizing and reducing thermal treatments. The problem addressed is of particular interest in relation to pillared structures obtained after preparing a PILC under reducing conditions. Finally the characterization of the nano-structure of these materials under redox conditions (e.g., in catalytic process), falls also in the focus of this work.

The study is based mainly on  $^{57}\text{Fe}$  Mössbauer spectroscopy which is a powerful analytical technique whenever iron is incorporated in materials. In the case of clays, most of which contain in their lattices Fe as substitution for Al or Si, this spectroscopy proved to be particularly helpful (Coey, 1980). With it, it is possible to identify the crystal sites of iron in the clay lattice as well as to characterize iron compounds, usually oxo-hydroxides, attached to the clay surfaces. Therefore, this technique is most appropriate for studying the iron phases present in the modified clays prepared in this work.

## EXPERIMENTAL

### Materials

The modified clays examined in this work were derived from a common PILC-precursor (sample code S1), supplied by Straton Hi-Tec Ltd. This precursor was prepared from a  $\text{Na}^+$ -montmorillonite, hereafter designated as sample S0, which possesses a cation exchange capacity of 95 meq/100 g. This clay was dispersed (2 wt. %) in water and then contacted twice with an intercalant solution containing equal amounts of Al and trivalent Fe chlorides ( $\text{Al/Fe} = 1/1$ ). Between the first and second contact the flocculated clay was separated by filtration and then re-dispersed in water. The end loading of the clay was about 6 mMol  $\text{M}^{3+}/\text{g-clay}$ . More specifically the intercalant solution, 0.4 M with respect to each of these metal ions, has been initially titrated with a 0.4 M NaOH water solution up to  $\text{pH} = 4.4$  and stayed clear to the end. The flocculated clay was first washed with acidified water of  $\text{pH} = 4$ , for removing any metal oxy-hydroxides that might have precipitated at the external clay surfaces. Then, three more washings followed with distilled water and finally the end clay derivative was dried at  $80^\circ\text{C}$  in air. Sample

S1, the PILC-precursor, was then subjected to a series of heat treatments under alternating oxidizing (air,  $500^\circ\text{C}$ , 3 hours) and reducing ( $\text{H}_2$  flow,  $500^\circ\text{C}$ , 3 hours) conditions. Ten different samples were obtained and are designated by the codes given in the diagram shown in Figure 1. The samples listed in the upper branch of the diagram were obtained by heating S1 first under oxidizing conditions, then under reducing, then again under oxidizing and so on. The samples listed in the lower branch of the diagram were obtained by heating S1 first under reducing conditions, then under oxidizing, then again under reducing and so on. At the end of each heat treatment, few hundred milli grams were removed from the starting mass.

Heating these materials at  $500^\circ\text{C}$ , while insufficient to produce significant transformations of the basic clay mineral structure, suffices to transform the intercalated Fe/Al moieties to their oxide forms.

### Analytical techniques

Elemental analyses of the starting clay (S0) and the PILC SO1 were performed at the N.C.S.R. "Demokritos," Athens, Greece, using the characteristic X- and  $\gamma$ -rays induced by  $\gamma$ -rays or protons (Karydas and Paradellis, 1990; Savidou and Paradellis, 1990). Powder X-ray diffraction patterns were obtained for all samples prepared, employing a Siemens D500 diffractometer and Cu-K $\alpha$  radiation. Specific surface area (SSA) values, with an estimated error less than 7%, were determined from  $\text{N}_2$  adsorption data at  $T = 77\text{ K}$  by employing BET single point method. A Carlo-Erba SORPTY 1750 apparatus was used for these measurements. The samples were first degassed for 3 hours at  $300^\circ\text{C}$  in a vacuum of  $10^{-2}$  mbar.

Mössbauer spectra were collected using a constant acceleration spectrometer with a  $^{57}\text{Co}$  source in Rh matrix. The spectrometer was calibrated with a natural iron foil (NBS #1541) at room temperature and isomer shift values are given relative to this. Spectra were collected in the temperature range 4.2 to 292 K and the experimental data were fitted by a least squares computer minimization using a sum of spectral components characterizing different iron phases (Longworth, 1984).

The catalytic reduction of NO by CO (Voorhoeve and Trimble, 1975) was conducted in a bench scale plug flow reactor. The reactants  $\text{NO}:\text{CO}:\text{CH}_4:\text{He} = 2:2:2:94$ , with a total flow 100 ml/min, were passing through the catalyst bed containing  $\sim 400$  mg of sample. The analysis of the reactants and products was carried out by Gas Chromatographer equipped with a Thermal Conductivity Detector. The separation of the gases was achieved at  $30^\circ\text{C}$  using a system of two columns, Porapak Q (ss.  $2\text{ m} \times 0.31\text{ mm}$ ) and Molecular Sieve 13X (ss.  $3\text{ m} \times 0.31\text{ mm}$ ), connected in series through a six port valve automatically activated by computer. The above system was necessary for analyzing  $\text{O}_2$ ,  $\text{N}_2$ ,

Table 1. Elemental analysis of well dried Na<sup>+</sup> montmorillonite (sample S0) and pillared clay SO1.

Element	S0	SO1
	Weight %	
Si	30.1	19.5
Al	9.1	13.2
Mg	1.7	1.3
Fe	2.5	19.5
Ti	0.2	0.1
K	0.65	0.11
Na	2.2	0.01
Ca	1.72	0.03

N<sub>2</sub>O, CO<sub>2</sub>, NO, CO and CH<sub>4</sub> simultaneously and gave highly reproducible results.

### RESULTS

The elemental analysis for samples S0 and SO1, presented in Table 1, shows that practically all Na<sup>+</sup> and Ca<sup>++</sup> ions as well as most of K<sup>+</sup> ions were replaced by the cationic complexes present in the intercalant solution. This fact is further corroborated by the increase of Al and Fe in SO1. A rough estimate of the amounts uptaken can be obtained by comparing the ratios of the gram atoms % of these two elements with respect to the gram atoms % of silicon. The comparison shows that these ratios are within less than 20% the same, Fe being more strongly uptaken. Thus, the elemental analysis clearly indicates that both metal ions, Al and Fe, have been uptaken by the clay in about equal proportion, i.e., as these were present in the intercalant solution.

The N<sub>2</sub> sorption-desorption data (see Table 2) and the XRD patterns give evidence that the heated derivatives of S1 have a pillared structure. More specifically, the values for the d<sub>001</sub>-spacings that were deduced from the XRD patterns start from 1.56 nm (for sample S1) and then diminish gradually to 1.26 ± 0.18 nm upon heating this material at 500°C, either under oxidizing or reducing conditions. A single test at 600°C in air showed that the 0.3 nm interlayer opening is stable even at this high temperature. This stable interlayer opening of about 0.3 nm, although small compared to values found in most PILCs, is still not unusual for a pillared clay (Endo *et al.*, 1980). Furthermore the SSA-values (~100 m<sup>2</sup>/g) measured for all SO- and SR-samples furnish additional support for envisaging these samples as clay structures with layers propped apart by pillars. Indeed, the aforementioned SSA values, although smaller than the typical values for PILCs with 1 nm high pillars, are much larger than the typical values (~20 m<sup>2</sup>/g) found for non-expanded montmorillonite. Furthermore these SSA-values compare well with the values found by Endo *et al.* (1980) for a montmorillonite with silica pillars 0.3 nm high. This comparison is sound, in view of the fact that in both

Table 2. BET specific surface area from single point measurements.

Sample	Area (m <sup>2</sup> g <sup>-1</sup> )	Sample	Area (m <sup>2</sup> g <sup>-1</sup> )
S0	19	S1	108
SO1	127	SR1	99
SO2	98	SR2	101
SO3	100	SR3	99
SO4	95	SR4	95
SO5	98	SR5	93

cases the interlayer opening is nearly the same. Furthermore the height of the pillars is comparable to the molecular diameter of the N<sub>2</sub>, which is 0.36 nm. This small interlayer opening leads to the rather small SSA-values characterizing the modified clays prepared in this work, as well as in the previously mentioned Si-pillared montmorillonite. Finally, a sharp pore size distribution centred around 3.5 nm was found for sample SO1, a fact corroborating also a pillar structure.

The Mössbauer spectra of all heated samples taken at 292 K can be divided into two groups. In the first group fall spectra with a dominant symmetric quadrupole doublet having hyperfine parameters (see Table 3) which correspond to paramagnetic Fe<sup>3+</sup> in octahedral co-ordination. This type of spectrum is characteristic for all samples obtained after a final oxidizing

Table 3. Mössbauer hyperfine parameters of pillared samples at room temperature.

Sample	I.S* (mm/s)	ΔE <sub>q</sub> * (mm/s)	H <sub>cr</sub> ** (T)	Area** (%)
SO1	0.34	0.92	—	100
SO2	0.37	0.95	—	35
	1.08	2.19	—	65
SO3	0.34	1.22	—	100
SO4	0.35–0.44	0.88	—	19
	1.07	2.20	—	75
	0	0	33.1	6 (α-Fe)
SO5	0.33	1.28	—	100
SR1	0.44	0.73	—	13
	1.07	2.24	—	80
	0	0	33.0	7 (α-Fe)
SR2	0.33	1.25	—	94
	0.37	-0.11	50.8	6 (α-Fe <sub>2</sub> O <sub>3</sub> )
SR3	0.35–0.44	0.86	—	21
	1.07	2.25	—	73
	0	0	33.1	6 (α-Fe)
SR4	0.34	1.32	—	93
	0.38	-0.11	50.9	7 (α-Fe <sub>2</sub> O <sub>3</sub> )
SR5	0.35–0.44	0.75	—	12
	1.07	2.20	—	80
	0	0	33.0	8 (α-Fe)

\* The estimated error is ±2 on the last significant figure.

\*\*The estimated error is ±5 on the last significant figure.

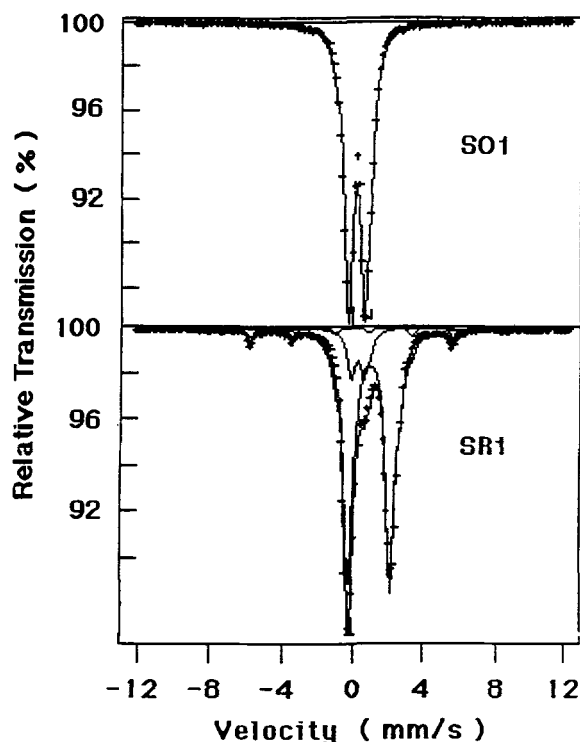


Figure 2. Representative Mössbauer spectra at 292 K of oxidized (SO1) and reduced (SR1) samples. Crosses denote experimental data. The result of the least squares fit as well as its spectral components are drawn by solid lines.

heating, i.e., for SO1, SR2, SO3, SR4 and SO5. The spectrum of SO1, typical for this group, is shown in Figure 2. The second group comprises the spectra for samples heated under reducing atmosphere, i.e., the spectra for SR1, SO2, SR3, SO4 and SR5. The spectrum for SR1, shown also in Figure 2, is typical for this group and consists of two paramagnetic components, a ferric and a ferrous (the doublet with the higher intensity), plus a weak magnetic component with hyperfine parameters corresponding to metallic iron. This latter component, however, has not been detected in the spectrum of SO2. A weak ( $\sim 6\%$ ) magnetic component (sextet), with hyperfine parameters corresponding to hematite ( $\alpha\text{-Fe}_2\text{O}_3$ ), is detected in the spectra of SR2 and SR4 samples belonging to the series that started by heating S1 in reducing atmosphere.

The Mössbauer spectra taken at 20 K (see Figure 3) are quite similar to those taken at 292 K and thus, the same grouping applies here too. The hyperfine parameters in Tables 3 and 4 corroborate further this similarity. The only exception refers to sample SO1, in the spectrum of which a dramatic change is observed between 292 K and 20 K. This change reveals, as will be elaborated in the Discussion below, that in this sample the iron oxide particles are definitely larger than in all other samples prepared out of S1.

For elucidating further the different iron phases in the aforementioned spectral groups, spectra were also obtained at 4.2 K. Figure 4 presents only three of these spectra and more specifically those corresponding to the PILC-precursor (S1) and to samples SO1 and SR1. A quite good fit of the spectrum for S1 was obtained with three ferric spectral components, one paramagnetic (doublet) and two magnetic sextets. The area of the paramagnetic component accounts for about 9% of the total spectral area. However, at 20 K this later component covers more than 90% of the total spectral area and at 292 K is the only spectral component present. The spectrum for sample SO1 at 4.2 K has been fitted in the same way and again the doublet at this temperature covers a clearly smaller area than in the 20 K spectrum. The 4.2 K spectra (not shown in Figure 4) for the other samples that went through a final oxidizing stage, have been analyzed as the SO1 spectrum, although their paramagnetic doublets are more intense. The third spectrum in Figure 4 is representative of the 4.2 K spectra for samples heated under reducing conditions. An acceptable analysis of these spectra would require more than one ferrous and one ferric magnetically splitted components. Such an analysis is very cumbersome and has not been carried out since it would not significantly add to the conclusions emerging from the spectral shapes per se (see below).

It is finally noted that the 292 K and 20 K spectra for sample S0 reveal the presence of the following iron phases, quite common in montmorillonites (Rozenon and Heller-Kallai, 1976): one paramagnetic ferric phase (85%) and one paramagnetic ferrous phase (15%), both octahedrally co-ordinated in the silicate lattice. The chemical analysis (Table 1) shows that the iron, initially present in the clay, is about 7 times less than the iron uptaken by the clay after intercalation. Therefore, the lattice iron cannot be detected in the spectra of the modified clay samples, although evidently it contributes too.

## DISCUSSION

The small, about 0.3 nm, opening of the clay layers in the PILCs prepared in this work indicates that the pillars along a direction perpendicular to the clay layers contain only one metal atom, Al or Fe. Although the diameter of the pillars cannot be directly determined, it should be finite in view of the high surface areas found in spite of the small interlayer opening. Thus, the presence of magnetic ordering observed at 4.2 K Mössbauer spectra for the PILC precursor (sample S1), as well as for the prepared PILCs, could be explained by magnetic bridging of these very thin "pancake" like pillars across the clay layers (Gangas *et al.*, 1987; Doff *et al.*, 1988). The BET surface area (see Table 2) has nearly the same value for all samples apart from SO1, which has  $\sim 30\%$  larger area. The catalytic activity of sample SO1 is also higher, by about 20%, than that of

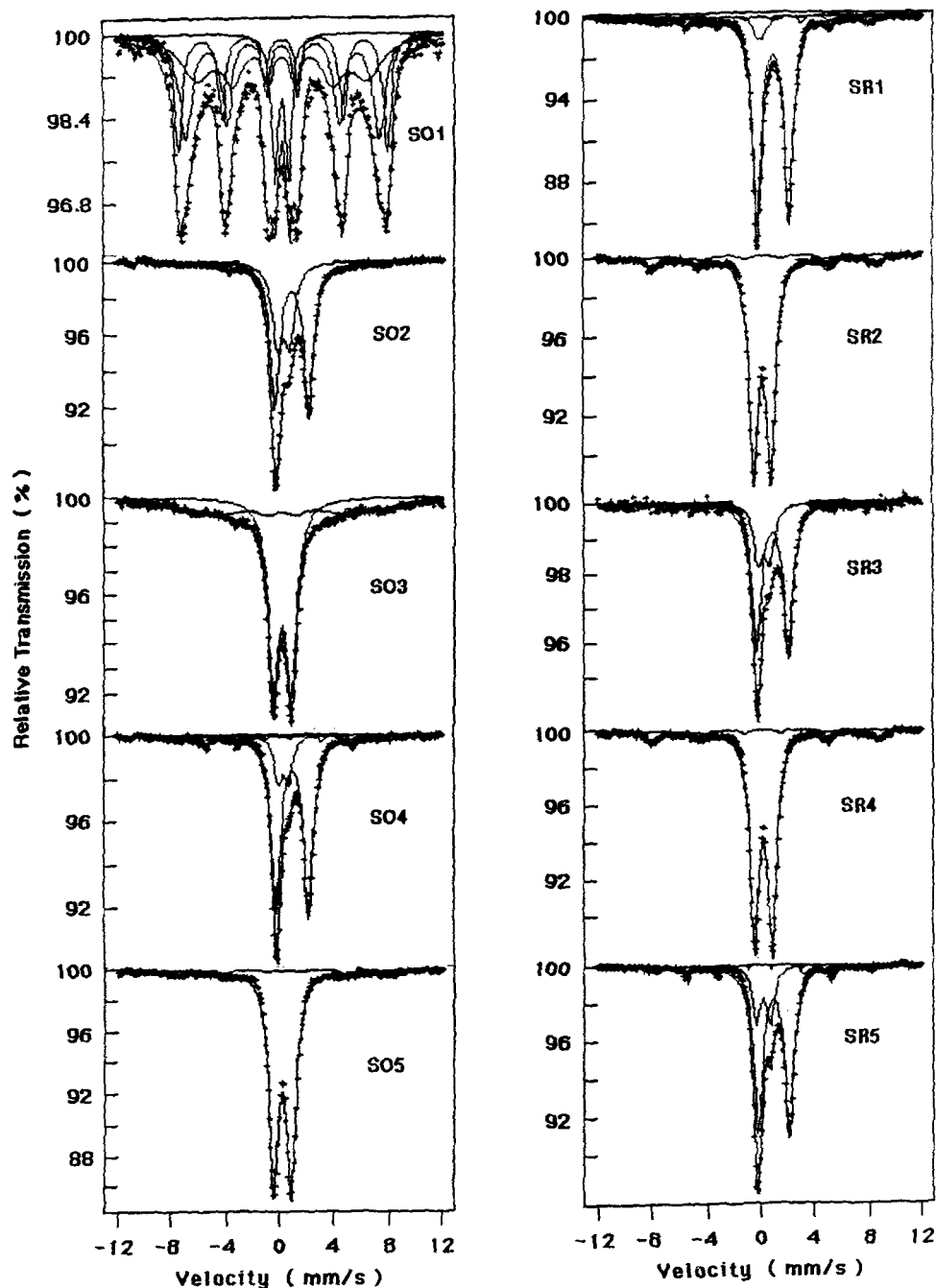


Figure 3. Mössbauer spectra at 20 K of oxidized and reduced samples. Crosses denote experimental data. The result of the least squares fit as well as its spectral components are drawn by solid lines.

all other samples as shown in Figure 5. The measured yield values are, however, generally small and this finding may indicate that the small interlayer opening hinders diffusion in the interlayer space.

Turning now to the discussion of the Mössbauer results, we first address the case of sample S1, i.e., the PILC precursor. In its 4.2 K spectrum there is a major magnetically splitted spectral component having val-

ues for hyperfine field ( $H_{\text{eff}} \leq 47.0\text{T}$ ) and for isomer shift ( $IS = 0.47\text{ mm/s}$ ) close to those given by Murad and Johnston (1987) for  $\gamma\text{-FeOOH}$  (lepidocrocite). The assignment of this magnetic component to  $\gamma\text{-FeOOH}$  might, however, look questionable because spectra of amorphous  $\text{Fe}_2\text{O}_3$  particles and  $\alpha\text{-Fe}_2\text{O}_3$  with Al substitutions give similar values of the hyperfine parameters. But sample S1 has not been heated in air at



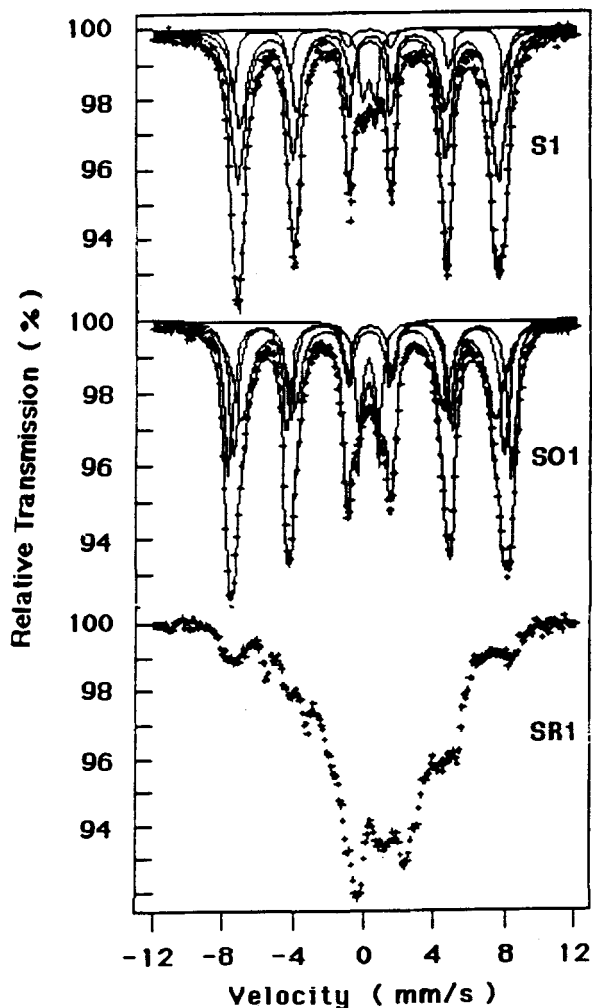


Figure 4. Mössbauer spectra at 4.2 K of PILC-precursor sample S1, oxidized sample SO1 and reduced sample SR1. The result of the least squares fit as well as its spectral components are drawn by solid lines.

temperatures above 80°C and therefore Fe oxide particles cannot be justified. The R.T. spectrum of this sample consists of only one paramagnetic doublet as expected for  $\gamma$ -FeOOH (Takada *et al.*, 1964). The high value of  $\Delta E_q = 0.72$  mm/s, found in the R.T. spectrum, is attributed to a severely distorted octahedral environment, due either to substitution of Al for Fe in the structure or/and to the small size of the Fe oxo-hydroxide particles.

Upon heating S1 in air at 500°C to obtain SO1, we envisage that the initially present Al substituted lepidocrocite converts into  $\gamma$ -(Fe<sub>1-c</sub>Al<sub>c</sub>)<sub>2</sub>O<sub>3</sub>. For pure lepidocrocite the transformation to maghemite ( $\gamma$ -Fe<sub>2</sub>O<sub>3</sub>) occurs already at 350°C. But it is also known from the results by De Villiers and van Rooyen (1967), that substitution of Al for Fe shifts the transformation to a higher temperature.

Table 4. Mössbauer hyperfine parameters of pillared samples at 20 K.

Sample	IS* (mm/s)	$\Delta E_q^*$ (mm/s)	$H_{\text{eff}}^{**}$ (T)	Area** (%)
SO1	0.44	1.08	—	15
	0.44	-0.02	46.4	61
	0.44	-0.02	40.2	23
SO2	0.40-0.50	0.89	—	36
	1.17	2.48	—	64
SO3	0.44	1.25	—	59
	0.44	0.03	43.5	41
SO4	0.40-0.50	0.82	—	19
	1.12	2.36	—	79
	0.11	0	33.4	2
SO5	0.44	1.27	—	93
	0.44	-0.04	47.7	7
SR1	0.40-0.50	0.67	—	8
	1.12	2.39	—	85
	0.11	0	33.4	7
SR2	0.44	1.27	—	90
	0.44	0.04	51.8	10
SR3	0.53	0.86	—	28
	1.16	2.37	—	72
SR4	0.44	1.31	—	90
	0.45	0.06	51.9	10
SR5	0.40-0.50	1.05	—	21
	1.20	2.31	—	73
	0.03	0	33.1	6

\* The estimated error is  $\pm 2$  on the last significant figure.

\*\* The estimated error is  $\pm 5$  on the last significant figure.

The R.T. spectrum of SO1 shows only one paramagnetic doublet, while at 20 K the spectrum consists of one paramagnetic component accounting for 15% of the total area of the spectrum and one magnetic component with asymmetrically broadened lines. This decrease of the area of the paramagnetic component and the compensating increase of the magnetic component points to superparamagnetism, a phenomenon emanating whenever the magnetic anisotropy energy of nano-sized particles of magnetically ordered phases (Morup, 1987) becomes comparable to the thermal energy  $kT$ . The superparamagnetic behavior of sample SO1 indicates that the diameter of the iron oxide species in the pillars, i.e., their extent along the interlayer, is only a few nanometers. This small lateral size of the particles and the substitution of Al for Fe in their structure may fully account for the high quadrupole splitting observed in SO1 and the other oxidized samples. Further support to this explanation furnishes the fact that the 4.2 K spectrum reveals the presence of a distribution of magnetic fields. Indeed, a good fitting of the magnetic part of this spectrum can be obtained by at least three spectral components. The values of isomer shifts and the average hyperfine fields of these components point out that the produced oxides in SO1 are probably small particles of  $\gamma$ -(Fe<sub>1-c</sub>Al<sub>c</sub>)<sub>2</sub>O<sub>3</sub>.

Major changes in the spectrum profile are observed

after heating sample S1 in reducing conditions (sample SR1). It is known (Terashima and Bando, 1985) that small particles of multilayered  $\alpha$ - $\text{Fe}_2\text{O}_3$ -SiO films, heated in a  $\text{H}_2$  atmosphere at  $250^\circ\text{C}$  for 1 hour, convert into small particles of  $\text{Fe}_3\text{O}_4$ -SiO. The hyperfine parameters of the R.T. spectrum of sample SR1 are very close to the parameters found by the aforementioned authors. The R.T. and 20 K spectra of SR1 can be analyzed by three spectral components: two doublets and one small magnetic component, attributed to metallic iron (Tables 3 and 4). The hyperfine parameters of the more intense doublet reveal the presence of divalent Fe in octahedral environment. The  $\Delta E_q$  value of the  $\text{Fe}^{2+}$  site increases as the temperature decreases, a typical behavior of  $\text{Fe}^{2+}$  in a distorted octahedral environment. The less intense doublet arises from  $\text{Fe}^{3+}$  in two sites, octahedral and tetrahedral. However, due to its small spectral contribution, only one doublet has been used to describe iron in both of these sites. At 4.2 K the spectrum is similar to that reported for  $\text{FeAl}_2\text{O}_4$  (Dormann *et al.*, 1990), apart from the fact that in the SR1 there is an extra spectral component in addition to the  $\text{Fe}^{2+}$  of  $\text{FeAl}_2\text{O}_4$ . Thus, the Mössbauer analysis suggests that the pillars of sample SR1 are identified as  $\text{Fe}_{3-x}\text{Al}_x\text{O}_4$ , where Fe atoms occupy the A and B sites of the magnetite structure.

Samples SO3, SO5, SR2, and SR4 produced after a final oxidizing heat treatment have also maghemitic pillars, as in SO1, but of smaller diameter. The superparamagnetic features of the 20 K spectra permit a classification with respect to the lateral size of the pillars. As it is clear from Table 4, the magnetic component in the case of sample SO3 accounts for 41% of the spectral area, while for the remaining samples for only  $\sim 10\%$ . Therefore, the sample SO3 has pillars with intermediate size between SO1, where 85% is magnetic, and the remaining oxidized samples. This is an interesting result because it shows that heating in  $\text{H}_2$  leads to the breaking down of the pillars to moieties with smaller diameter. The fact that any following oxidizing step does not sinter these moieties to pillars with larger diameters is explained by our assumption that the  $\text{Fe}^{3+}$  ions uptaken from the intercalated solution occupy the interlayer space. If the Fe oxides were covering the outer surface of the clay platelets, their size would increase by sintering during firing in air (Simopoulos *et al.*, 1975). The deduced decrease of the lateral size of these oxide particles is probably due to a reorganization of their crystallographic structure upon the reduction of  $\text{Fe}^{3+}$  to  $\text{Fe}^{2+}$ . However, this decrease may be at least partly due to a decrease of the apparent "magnetic size." This can result from a pinning of some surface  $\text{Fe}^{3+}$  spins and leads to a superparamagnetic behavior that hints to smaller particle sizes (Morup, 1987).

As in the case of SR1, the samples SR3, SR5, SO2 and SO4, that were also gained after a final reducing

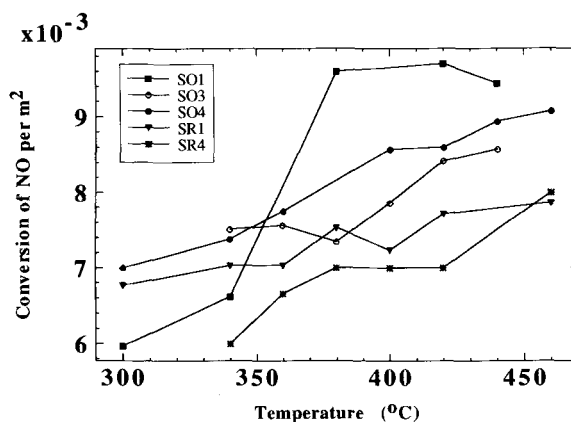


Figure 5. Yield of the reaction  $\text{CO} + \text{NO}$  performed on the samples shown. Solid lines have been drawn as eye guide and they do not infer any functional dependence.

heating, have pillars consisting of Al-substituted magnetite. However, the analysis of the corresponding spectra showed significant changes with respect to the areas of the spectral subcomponents. Especially from data at R.T. (Table 3), it is clear that the area of the ferric component increases. Two paramagnetic spectral components, one for  $\text{Fe}^{3+}$  and one for  $\text{Fe}^{2+}$  are necessary to fit the formed magnetite phase, although due to Al substitutions, electron delocalization on the octahedral sites becomes inhibited, and two  $\text{Fe}^{3+}$  subspectra are expected (Annersten and Hafner, 1973). The presence of only one ferric doublet for the tetrahedral and octahedral occupancy having larger width and intermediate value for the quadrupole splitting parameter supports the assumption that what one actually measures is a weighted average of trivalent iron distributed in the available positions. The slightly larger values for isomer shifts may indicate variations in the s-electron density at the nucleus site.

## SUMMARY

Thus, on the basis of the Mössbauer spectra, we may draw the following conclusions with respect to the chemical composition and morphology of the pillars:

- 1) Firing in air transforms the intercalated lepidocrocite into Al-substituted maghemite, whereas heating in  $\text{H}_2$  atmosphere transforms the lepidocrocite into Al-substituted magnetite. The temperature dependence of the Mössbauer spectra indicates that the diameter of these oxide particles is smaller than  $\sim 10$  nm (Morup *et al.*, 1980).

- 2) Samples that went through a reducing heat treatment, either at the beginning or at a later stage, end up with broken pillars which do not sinter during subsequent oxidizing stages.

Furthermore, the present work reveals that cyclic redox heat treatments of smectites intercalated with iron-complexes furnish a new route for changing the

morphology of the inserted nanoparticle materials. Clearly, Mössbauer spectroscopy furnishes a unique tool for following these transformations.

#### ACKNOWLEDGMENTS

Thanks are due to A. Savidou, A. G. Karydas and T. Paradellis (NCSR "Demokritos," Athens, Greece) for the elemental analysis of samples given in Table 1, to the NCSR "Demokritos" Mössbauer group (A. Simopoulos and A. Kostikas) for providing liquid He facilities and D. Petrides for his valuable comments. This work has been partially supported by the Commission of the European Communities under the Brite-Euram Programme "Concerted European Action on Pillared Layered Structures."

#### REFERENCES

- Annersten, H. and Hafner, S. S. (1973) Vacancy distribution in synthetic spinels of the series  $\text{Fe}_3\text{O}_4\text{-}\gamma\text{-Fe}_2\text{O}_3$ : *Z. Kristallogr.* **137**: 321–340.
- Bartley, G. J. J. (1988) Zirconium pillared clays: *Catal. Today* **2**: 233–241.
- Bergaya, F. and Barrault, J. (1990) Mixed Al-Fe pillared laponites: Preparation characterization and their catalytic properties in syngas conversion: in *Pillared Layered Structures: Current Trends and Applications*: I. V. Mitchell, ed., Commission of European Communities, Elsevier Applied Science, London, 167–184.
- Bergaya, F., Hassoun, N., Gatineau, L., and Barrault, J. (1991) Mixed Al-Fe pillared laponites: Preparation, characterization and catalytic properties in syngas conversion: in *Preparation of Catalysts V*: G. Poncelet, P. A. Jacobs, P. Grange, and B. Delmon, eds., Elsevier Science Publishers B. V., Amsterdam, 329–337.
- Bergaya, F., Hassoun, N., Barrault, J., and Gatineau, L. (1993) Pillaring of synthetic hectorite by mixed  $[\text{Al}_{1-x}\text{Fe}_x]$  pillars: *Clay Miner.* **28**: 109–122.
- Braddell, O., Barklie, R. C., Doff, D. H., Gangas, N. H. J., and McKimm, A. (1987) EPR of  $\text{Cu}^{2+}$  ions in pillared clay: *Zeit. Phys. Chem.* **151**: 157–164.
- Brindley, G. W. and Sempels, R. E. (1977) Preparation and properties of some hydroxy-aluminium beidellites: *Clay Miner.* **12**: 229–236.
- Coey, J. M. D. (1980) *At. Energy Rev.* **18**: no. 1, 73–124.
- Christiano, S. P. and Pinnavaia, T. J. (1986) Intercalation in montmorillonite of molybdenum cations containing the  $\text{Mo}_6\text{Cl}_8$  cluster core: *J. Solid State Chem.* **64**: 232–239.
- Christiano, S. P., Wang, J., and Pinnavaia, T. J. (1985) Intercalation of Niobium and Tantalum  $\text{M}_6\text{Cl}_{12}^{n+}$  cluster cations in montmorillonite: A new route to pillared clays: *Inorg. Chem.* **24**: 1222–1227.
- De Grave, E., Bowen, L. H., and Weed, S. B. (1982) Mossbauer study of Aluminum-substituted hematites: *J. Mag. Mat.* **27**: 98–108.
- De Villiers, J. M. and van Rooyen, T. H. (1967) Solid solution formation of lepidocrocite-boehmite and its occurrence in soil: *Clay Miner.* **7**: 229–235.
- Doff, D. H., Gangas, N. H. J., Allan, J. E. M., and Coey, J. M. D. (1988) Preparation and characterization of iron oxide pillared montmorillonite: *Clay Miner.* **23**: 367–377.
- Dormann, J. L., Seqqat, M., Fiorani, D., Nogues, M., Soubeyroux, J. L., Bhargava, S. C., and Renaudin, P. (1990) Mössbauer studies of  $\text{FeAl}_2\text{O}_4$  and  $\text{FeIn}_2\text{S}_4$  spin glass spinels: *Hyper. Inter.* **54**: 503–508.
- Endo, T., Mortland, M. M., and Pinnavaia, T. J. (1980) Intercalation of silica in smectites: *Clays & Clay Minerals* **28**: 105–110.
- Fripiat, J. J. (1986) Internal surface of clays and constrained chemical reactions: *Clays & Clay Minerals* **34**: 501–506.
- Gangas, N. H. J., van Wonerghem, J., Morup, S., and Koch, C. J. W. (1985) Magnetic bridging in nontronite by intercalated iron: *J. Phys. C* **18**: L1011–L1015.
- Gangas, N. H., Bakas, T., Moukarika, A., Petrides, D., and Simopoulos, A. (1987) Magnetic ordering in nontronite pillared with Al-polyoxo cations: *NATO ASI Chemical Physics of Intercalation*, Castera-Verduzan, France.
- Harsh, J. B. and Doner, H. E. (1984) Specific adsorption of copper on an hydroxy-aluminium-montmorillonite complex: *Soil Sci. Am. Proc.* **48**: 1034–1039.
- Karydas, A. G. and Paradellis, T. (1990) Coal XRF analysis using a proton induced copper X-ray beam: *J. Coal Qual.* **9**: no. 2, 39–43.
- Lahav, N., Shani, U., and Shabtai, J. (1978) Cross-linked smectites. I—Synthesis and properties of hydroxy-aluminium-montmorillonite: *Clays & Clay Minerals* **26**: 107–115.
- Longworth, G. (1984) Spectral data reduction and refinement: in *Mössbauer Spectroscopy Applied to Inorganic Chemistry, Vol. 1*, G. J. Long, ed., Plenum Press, New York and London, 43–56.
- Lee Woo, Y., Raythatha, R. H., and Tatarchuk, B. J. (1989) Pillared-Clay Catalysts Containing Mixed-Metal Complexes: *J. Catal.* **115**: 159–179.
- Mitchell, I. V. (1990) ed. *Pillared Layered Structures. Current Trends and Applications*: Commission of European Communities, Elsevier Applied Science, London, 209–217.
- Morup, S. (1987) Mössbauer effect studies of microcrystalline materials: in *Mössbauer Spectroscopy Applied to Inorganic Chemistry, Vol. 2*, G. J. Long, ed., Long, Plenum Press, New York and London, 89–119.
- Morup, S., Dumesic, J. A., and Topsøe, H. (1980) Magnetic microcrystals: in *Applications of Mössbauer Spectroscopy, Vol. 2*, R. Cohen, ed., Academic Press, New York.
- Murad, E. and Johnston, H. J. (1987) Iron oxides and hydroxides: in *Mössbauer Spectroscopy Applied to Inorganic Chemistry, Vol. 2*, G. J. Long, ed., Plenum Press, New York and London, 507–574.
- Occelli, M. L. (1983) Catalytic cracking with an interlayered clay. A two-dimensional molecular sieve: *Ind. Eng. Chem. Prod. Res. Dev.* **22**: 553–559.
- Petrides, D., Bakas, T., Simopoulos, A., and Gangas, N. H. (1989) Pillaring of montmorillonite by organotin cationic complexes: *Inorg. Chem.* **28**: 2439–2443.
- Pinnavaia, T. J. (1983) Intercalated clay catalysts: *Science* **220**: 365–371.
- Pinnavaia, T. J., Rainey, V., Ming-Shin Tzou, and White, J. W. (1984) Characterization of pillared clays by neutron scattering: *J. Mol. Catal.* **27**: 213–224.
- Plee, D., Borg, F., Gatineau, L., and Fripiat, J. J. (1985) High resolution solid state  $^{27}\text{Al}$  and  $^{29}\text{Si}$  nuclear magnetic resonance study of pillared clays: *J. Amer. Chem. Soc.* **107**: 2362–2369.
- Rozenon, I. and Heller-Kallai, L. (1976) Reduction and oxidation of  $\text{Fe}^{3+}$  in dioctahedral smectites—1: Reduction with hydrazine and dithionite: *Clays & Clay Minerals* **24**: 271–282.
- Savidou, A. and Paradellis, T. (1990) Determination of light elements in a natural coal sample by PIGE spectroscopy: *J. Coal Qual.* **9**: no. 2, 45–47.
- Simopoulos, A., Kostikas, A., Sigalas, I., Gangas, N. H., and Moukarika, A. (1975) Mössbauer study of transformations induced in clays by firing: *Clays & Clay Minerals* **23**: 393–399.
- Sterte, J. (1986) Synthesis and properties of titanium oxide



- cross-linked montmorillonite: *Clays & Clay Minerals* **34**: 658–664.
- Takada, T., Kiyama, M., Bando, Y., Nakamura, T., Shiga, M., Shinjo, T., Yamamoto, N., Endoh, Y., and Takaki, H. (1964) Mössbauer study of  $\alpha$ -,  $\beta$ -, and  $\gamma$ -FeOOH: *J. Phys. Soc. Japan* **19**: 1744.
- Terashima, T. and Bando, Y. (1985) Magnetism of ultrathin Fe<sub>3</sub>O<sub>4</sub> films: *J. Phys. Soc. Japan* **54**: no. 10, 3920–3924.
- Tzou, M. S. and Pinnavaia, T. J. (1988) Chromia pillared clays: *Catal. Today* **2**: 243–259.
- Tillak, D., Tennakoon, B., Jones, W., and Thomas, J. M. (1986) Structural aspects of metal-oxide-pillared sheet silicates: *J. Chem. Soc., Faraday Trans. I* **82**: 3081–3095.
- Vaughan, D. E. W. (1988) Recent developments in pillared interlayered clays: in *Perspectives in Molecular Sieve Science, ACS Symposium Series* **368**: 308–323.
- Vaughan, D. E. W. and Lussier, R. J. (1980) Preparation of molecular sieves based on pillared interlayered clays: in *Proc. 5th International Conference on Zeolites, Naples*, L. V. C. Rees, ed., Heyden, London, 94–101.
- Voorhoeve, R. J. H. and Trimble, L. E. (1975) Reduction of nitric oxide with carbon monoxide and hydrogen over Ruthenium catalysts: *J. Catal.* **38**: 80–91.
- Yamanaka, S., Doi, T., Sako, S., and Hattori, M. (1984) High surface area solids obtained by intercalation of iron oxide pillars in montmorillonite: *Mat. Res. Bul.* **19**: 161–168.

(Received 13 April 1993; accepted 22 March 1994; Ms. 2362)